Journal of Power Sources 208 (2012) 440–446

Contents lists available at SciVerse ScienceDirect

Journal of Power Sources

journal homepage: www.elsevier.com/locate/jpowsour

On the synthesis conditions for tailoring lithium composition in ramsdellite phases: Application for Li-ion batteries

A. Soares, B. Fraisse, F. Morato, C.M. Ionica-Bousquet, L. Monconduit*

Institut Charles Gerhardt Montpellier, UMR 5253 CNRS, Université Montpellier 2, 34095 Montpellier, France

ARTICLE INFO

Article history:
Received 12 October 2011
Received in revised form
15 November 2011
Accepted 6 December 2011
Available online 16 December 2011

Keywords:
Titanates
Ramsdellitte
Synthesis
Carbonaceous precursor
Gas flow
Li ion battery

ABSTRACT

TiO_2 with the ramsdelitte-type (R) structure has a potential use as negative electrode for Li-ion battery due to its high theoretical capacity (335 mAh g^{-1}), a weak irreversible loss during the first cycle and a low polarization. However due to its metastability, TiO_2 (R) has been rarely reported. In the present work we report on the carbothermal synthesis of some Li_xTiO_2 delithiated R phases ($0 < x < 0.57$), from TiO_2 to $Li_2Ti_3O_7$, with ramsdellite-type structure. The variation of the synthesis parameters such as wt% of carbonaceous additive and reductive gas flow has conducted to the formation of poor lithiated Li_xTiO_2 phases and Li_2TiO_3 as additional phase. Their ratio was found to be strongly dependent on the amount of carbonaceous precursor. These new Li_xTiO_2(R)/Li_2TiO_3 composites (with ($0 \le x \le 0.57$)) were characterized by chemical analysis, X-ray diffraction and thermogravimetric analysis and finally by electrochemical tests. High capacities as well as good cycleability have been reached.

1. Introduction

Due to a good cycleability, a weak irreversible loss during the first cycle and a low polarization the lithiated titanates are good candidates as negative electrode material of Li-ion batteries. These materials are based on the redox couple Ti^{4+}/Ti^{3+} including a high working potential versus lithium (>1.5 V) which improve the safe conditions of use. In lithiated titanates, titanium is octahedrally coordinated by oxygen to build up the three dimensional framework of the oxide, leaving empty sites available for lithium insertion. For the ramsdellite (R) structure [1], the double columns of MO_6 octahedra (Fig. 1) lead to a rather open framework structure with tunnels, which are partly occupied by lithium in the case of $Li_{0.5}TiO_2$ [2], $Li_2Ti_3O_7$ [3] and lithium-free for TiO_2 (R) [2].

The ramsdellite $Li_2Ti_3O_7$ has been less investigated [4] than the other titanates, probably due to (i) the lithium insertion hold up by the presence of lithium in the structure and (ii) the limitation of the oxidation process due to Ti which is already in its highest oxidation state leading to low capacity. To increase in capacity few synthesis routes have been recently reported for preparing ramsdellite-type delithiated Li_xTiO_2 phases. $Li_{0.5}TiO_2$ (R) has been obtained by thermal treatment of the spinel $LiTi_2O_4$ at high temperature [5] and the lithium free TiO_2 (R) has been prepared by complex chemical delithiation from ternary compounds like hollandite, ramsdellite or spinel [6]. Poor lithiated phases have also been obtained by topotactic oxidation in air at room temperature of the lithium titanate bronze Li_xTiO_2 ($x = 0.41, 0.16, 0.14$) crystals with the ramsdellite-type structure with decreased unit cell volumes (vs $Li_2Ti_3O_7$) [6].

The preparation of the metastable TiO_2 (R) phase is still a challenge since the associated theoretical capacity is 335 mAh g^{-1} corresponding to the formation of Li_1TiO_2 and based upon the redox couple $Ti^{4+} \rightarrow Ti^{3+}$ working has never been reached. Moreover the reversible lithium insertion in TiO_2 (R) follows a topotactical mechanism which is generally associated with a limited electrode volume change.

Recently an original carbothermal synthesis route has led to a partially delithiated $Li_{2-x}Ti_3O_7$ (R) with $x < 2$ showing a specific capacity of 198 mAh g^{-1} close to the theoretical capacity of $Li_{2-x}Ti_3O_7$ [7]. In this previous work we demonstrated the impact of the nature of the gas during the synthesis on the nature of the composite. Note that a unique low gas flow was used and correlatively the ramsdellite phase was only partially delithiated.

In this work, the "in situ" preparation of delithiated Li_xTiO_2 (R) ($0 \le x \le 0.57$) by using carbothermal synthesis is presented. Under these specific conditions, the stabilization of TiO_2 (R) phase was achieved. The variation of the synthesis parameters such as temperature, gas flow and carbonaceous precursor amount and their influence on the purity of the as obtained composites are discussed. These new composite materials are characterized by X-ray diffraction, chemical and thermogravimetric analysis, as well as electrochemical measurements.

* Corresponding author. Tel.: +33 467 14 33 35; fax: +33 467 14 33 04.
E-mail address: laure.monconduit@univ-montp2.fr (L. Monconduit).

0378-7753/$ – see front matter © 2012 Elsevier B.V. All rights reserved.
doi:10.1016/j.jpowsour.2011.12.013

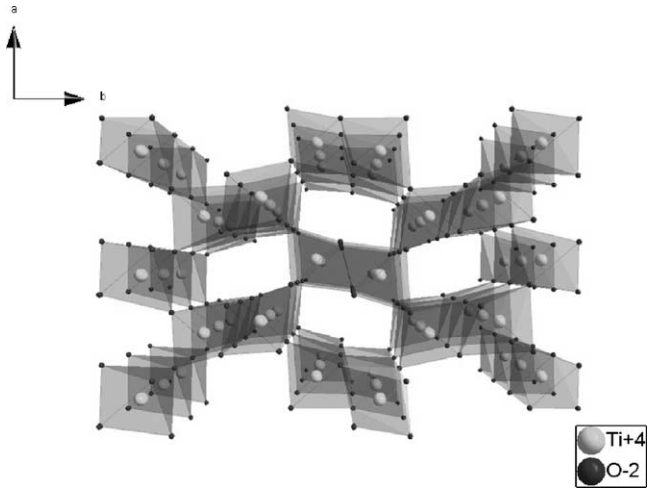

Fig. 1. Perspective view of the ramsdellite structure viewed along *c*, showing the empty sites in the channels created by the connections between TiO_6 polyhedrons. The small circles represent Ti atoms, the bigger represent O atoms.

2. Experimental

2.1. Synthesis procedure

Titanate composites have been prepared using a ceramic synthesis route including Li_2CO_3 (UMICORE, grain size ~40 μm) and TiO_2 (UMICORE, 45% anatase, 55% rutile, grain size ~20 μm) following the reaction (1).

$$Li_2CO_3 + 3TiO_2 \rightarrow Li_2Ti_3O_7 + CO_2 \quad (1)$$

Sucrose has been added as carbonaceous precursor with different percentages of weight (S or S′%) and the as obtained composites will be named hereafter S- or S′ samples depending on the gas flow used. The reagents were firstly homogeneously ground by planetary ball milling and, then, heated at 980 °C for 90 min under controlled atmosphere of Argon/Hydrogen (95/5%) in a furnace (79300 Thermolyne Tube Furnace). 0.5 and 0.05 L min^{-1} gas flows were used (S and S′ samples respectively). At the end of the heating period, the furnace was opened to rapidly cool the sample to room temperature (the sample under controlled atmosphere during this step) in order to stabilize the ramsdellite structure.

2.2. Chemical analysis and structure determination

The morphology of the S-samples was studied using a scanning electron microscope (Hitachi S-4800).

In order to determinate the amount of carbon in each sample, an analysis by combustion was applied. The residual carbon tenor was evaluated by a Flash EA 1112 analyzer based on the Dynamic Flash Combustion which produced complete combustion of the samples followed by an accurate and precise determination of the elemental gases produced.

The S-samples were analyzed by X-ray diffraction (XRD) (PHILIPS X'Pert MPD equipped with the X'celerator detector θ–2θ diffractometer) by using Cu Kα radiation (λ = 1.5418 Å) and a nickel filter. Structural refinements were carried out using the Debye and Rietveld methods with the Fullprof software suite [8].

Differential thermal analysis (DTA) was used in order to determine the different phase transformations by using a calorimeter SETARAM Thermogravimetric Analyzer (France). The measurements were done with 15 mg of the powder sample and data were collected under air flow between 300 and 1000 K, with heating and cooling rates of 15 K min^{-1}.

2.3. Electrochemical lithium insertion–deinsertion

Swagelok™-type cells were assembled in an argon filled glove box and cycled using a VMP automatic cycling/data recording system (Biologic Co, Claix, France) in a potential window between 2.5 V and 1.0 V vs Li^+/Li^0 and with a cycling rate of *C*/10 (that is one lithium per formula unit in 10 h). These cells comprise a Li_{metal} disc (Sigma–Aldrich) as the counter electrode. A Whatman GF/D borosilicate glass fiber separator sheet was saturated with a solution of 1 M $LiPF_6$ in ethylene carbonate (EC), propylene carbonate (PC), dimethyl carbonate (DMC) (1:1:3 v/v + 1% vinylenecarbonate (vc)) as the electrolyte. A working electrode was made by mixing the starting titanate powder with 15% (weight) carbon black.

3. Results and discussion

3.1. Morphological, chemical and structural analyses

Scanning electron microscopy (SEM) images in Fig. 2a and b show the S- and S′-samples prepared under 0.5 or 0.05 L min^{-1} of Ar/H_2 flows respectively. S-0- and S′-0-samples present shapeless crystallized grains of $Li_2Ti_3O_7$ R phase with a size ranging from 1 to 5 μm whatever the Ar/H_2 output used. When the amount of sucrose is increased in the synthesis from S-0 (S′-0) to S-15 (S′-15), smaller grains from 100 to 500 nm attributable to C appear mixed with the more crystallized grains of the R phase. No clear morphology differences are underlined between the samples prepared under low (S′) and high gas flow (S).

Table 1 shows the weight % C after combustion and the refined cell parameters of different S- and S′-samples prepared under 0.5 or 0.05 L min^{-1} of Ar/H_2 flows.

Only few amount of C in the range of 0.1–14% is kept in the various samples whatever the gas flow used. The refined cell parameters of both S′-0 and S′-15 prepared under low Ar/H_2 flow (0.05 L min^{-1}) are very close to those of the R reference and with higher carbonaceous amounts (S′-30, 40, 50) the cell parameters are slightly modified and previously given in a referenced paper.[7]

Fig. 3a shows the X-ray diffraction patterns of the S-samples prepared under 0.5 L min^{-1} flow (for clarity the 0.05 L min^{-1} are not

Table 1
X-ray refined cell parameters of the different S-samples synthesized under Ar/H_2 with various S weight% of sucrose. The weight % of the residual C is also given.

Ar/H_2 output	Samples	%C	% weight sucrose	*a* (Å)	*b* (Å)	*c* (Å)
	[JCPDS 00-034-0393]	–	0	5.018(1)	9.552(1)	2.945(1)
0.05 LPM	S′-0	0.1	0	5.001(1)	9.5492(1)	2.945 (1)
0.05 LPM	S′-15	2.1	15	4.997(1)	9.496 (1)	2.945(1)
0.5 LPM	S-0	0.3	0	5.017(1)	9.591(1)	2.948(1)
0.5 LPM	S-10	2.1	10	4.954(1)	9.450(1)	2.945(1)
0.5 LPM	S-15	2.8	15	4.917(1)	9.451(1)	2.950(1)
0.5 LPM	S-30	5.5	30	4.854(1)	9.437(1)	2.961(1)
0.5 LPM	S-40	9.2	40	4.835(1)	9.418(1)	2.963(1)
0.5 LPM	S-50	14.0	50	4.854(1)	9.454(2)	2.967(1)

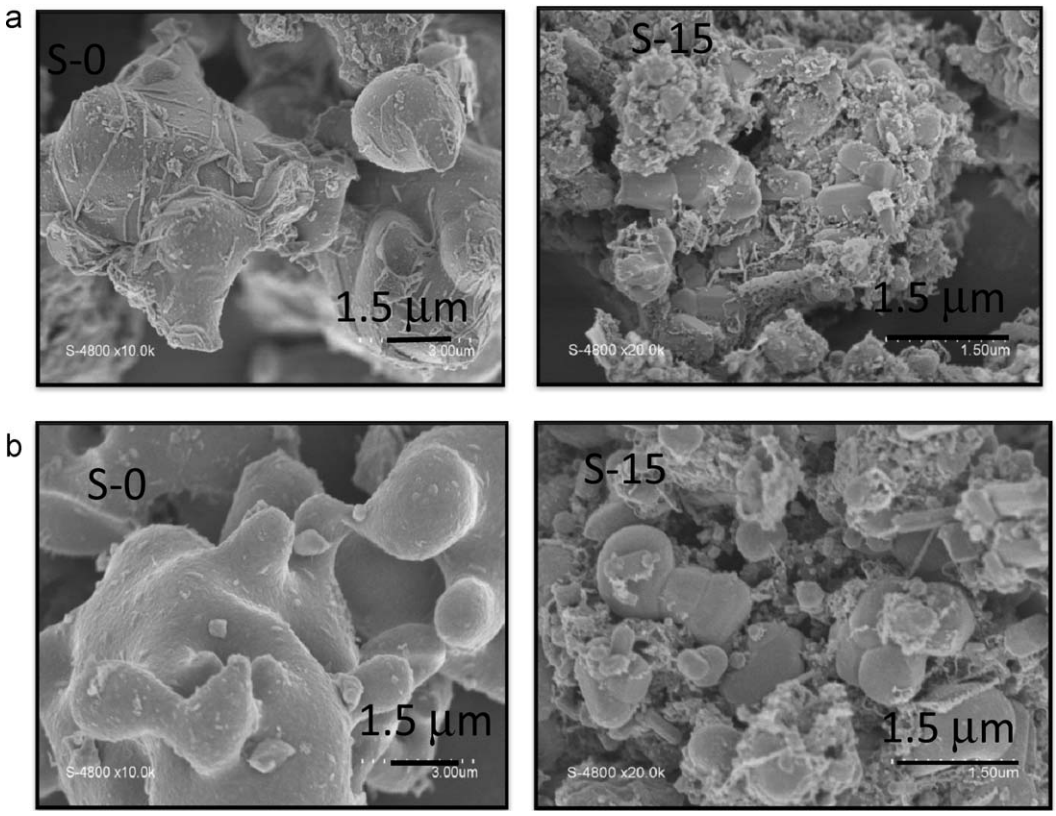

Fig. 2. SEM images of S-0 and S-15 prepared under (a) 0.5 L min^{-1} and (b) 0.05 Ar/H_2 flow.

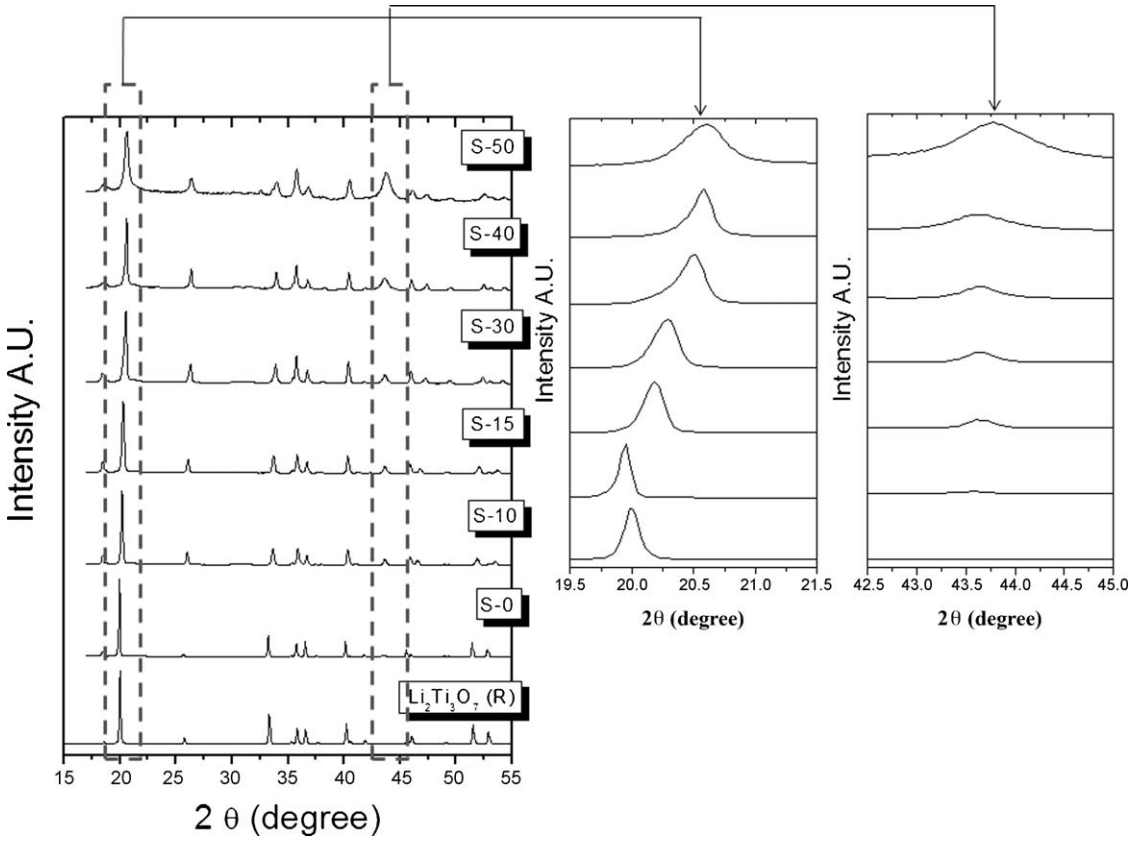

Fig. 3. X-ray diffraction patterns of S-samples in the 15–55° (2θ) range and magnified in the 19.5–21.5 and 42.5–45 (2θ) range.

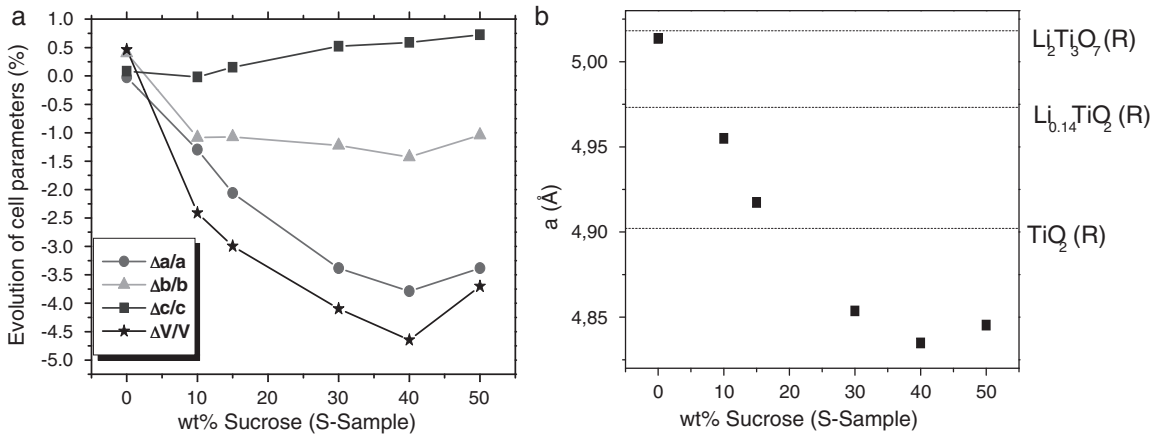

Fig. 4. (a) Evolution of cell parameters ($\Delta a/a$, $\Delta b/b$, $\Delta c/c$) in % for the S-samples ($0 < S < 50$) and (b) a parameter of S-samples as function of wt% sucrose used in the synthesis. The a parameters for Li_xTiO_2 ($x = 0.57$, 0.14 and 0) reference are reported on the graph.

presented in Fig. 3) and that of the standard ramsdellite $Li_2Ti_3O_7$ ($a = 5.018$ Å, $b = 9.552$ Å, $c = 2.945$ Å in *Pbnm* space group [JCPDS 00-034-0393]) as reference. Fig. 3b presents the magnified plot ($19.5 < 2\theta < 21.5^\circ$) of the XRD pattern of S-samples. The XRD patterns of all samples present Bragg peaks characteristics of the $Li_2Ti_3O_7$ ramsdellite type phase (R). The peaks attributed to this R phase are sharp in S-0 indicative of a high crystallinity and become broader in samples with increasing amount of sucrose in the synthesis indicative of an amorphisation of the sample or a C coating. More the amount of the residual C increases (from 0.3 to 14 wt%) in the sample more the Bragg peaks of the ramsdellite are shifted towards higher angles. Simultaneously, a broad peak appears at 43.7° (2 theta angles) which could be attributed to the [2 0 0] diffraction plan of the cubic phases Li_2TiO_3 [JCPDS 00-003-1024].

Fig. 4a gives the variation of the cell parameters of the R phase (given in Table 1) in S-samples as function of the amount of sucrose added during the synthesis. More the amount of sucrose added during the synthesis (S) increases (more the C content increases in the samples), more both a and b cell parameters decrease, while the c cell parameter is much less modified. The decrease in the a and b parameters leads to a volume decrease (V). The ramsdellite (R) framework consists in TiO_6 double rutile chains along the [0 0 1] direction, which are interconnected through corners in the ab plane (see Fig. 1). In the ramsdellite structure, the channels (parallel to the c axis) are partly occupied by lithium in the case of $Li_2Ti_3O_7$ [3] and empty in the case of TiO_2 (R) [7] and consequently a and b parameters decrease with decreasing the lithium content. Fig. 4b presents the refined a parameter of the S-samples. The comparison with the a parameters, $a = 5.018(1)$ Å, $a = 4.97(1)$ Å, $a = 4.902(1)$ Å reported for $Li_2Ti_3O_7$ and Li_xTiO_2 (R) ($x = 0.14$ and 0) respectively shows that the lithium content in the R phase decreases with increasing of C content in the S samples suggesting that the C has a structural influence on the R phase. The a parameters reach a minimum for the S-40 sample (containing 9.2% C). Note that the S-40 sample refined parameters $a = 4.835(2)$ Å, $b = 9.418(1)$ Å, $c = 2.963(1)$ Å are close to and even smaller than those referenced for TiO_2 (R) prepared by soft chemical technique (*Pbnm* with $a = 4.902(1)$ Å, $b = 9.459(1)$ Å, $c = 2.958(1)$ Å) [2,6].

3.2. Differential thermal analysis

Fig. 5 shows the DSC curve of the heating process under air obtained for the $Li_2Ti_3O_7$ reference, as well as for the S-15 and S-40 samples. The reference sample $Li_2Ti_3O_7$ gives only a sharp peak at 770 K characteristic of the orthorhombic- into hexagonal-$Li_2Ti_3O_7$ phase transition. For the S-15 and S-40 samples, after an endothermic peak due to desorption of surface water molecules, two sharp exothermic peaks can be seen at around 530 K and 640 K. The latter has been identified previously as being the transformation of TiO_2 (R) into the brookite-type TiO_2 [6]. Recently both structural stability and phase transition of TiO_2 (R) upon heating were investigated by XRD and DSC measurements and the peaks at 530 K was attributed to a TiO_2 ramsdellite-intergrowth phase transition and that at 640 K to the inter-growth–rutile transition [9]. This may be associated with the continuous structural changes from the TiO_2 ramsdellite to the TiO_2 rutile structure. In conclusion, the DSC curves confirm that the delithiated TiO_2 (R) is the main phase in the S-15 and S-40 samples.

3.3. Electrochemical performances

3.3.1. $Li_2Ti_3O_7$ (R)

Fig. 6a shows the galvanostatic curves of the various S-samples. The curve of the S-0, namely $Li_2Ti_3O_7$ (R) shows two distinct regions from 2.5 to 1.5 V and from 1.5 to 1 V. Previous studies have proposed that Li ions occupy two different kinds of tetrahedral sites in the tunnel, named T1 and T2 [10,11] with T1 sites more energetic stable than T2, because the corresponding LiO_4 tetrahedron does not share faces to any (Li, Ti)O_6 framework octahedron. Lithium ions located in the channels are distributed as follows: 60% over the more stable so-called T1 and 40% over the less stable so-called T2 site. In the

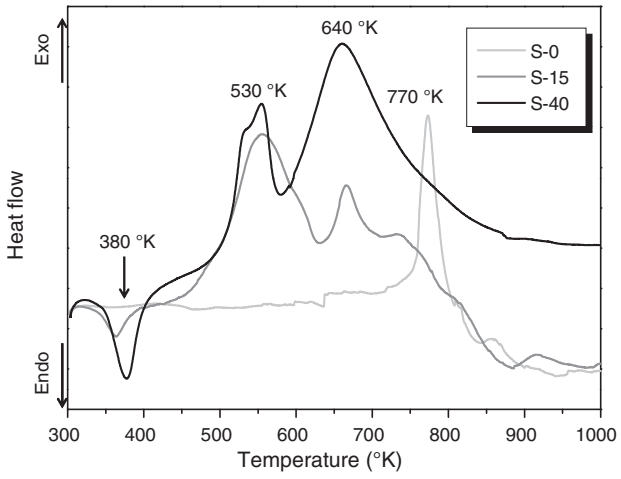

Fig. 5. Differential thermal analysis (10 °C min^{-1}) of S-samples (S-0 ($Li_2Ti_3O_7$), S-15 and S-40) under air.

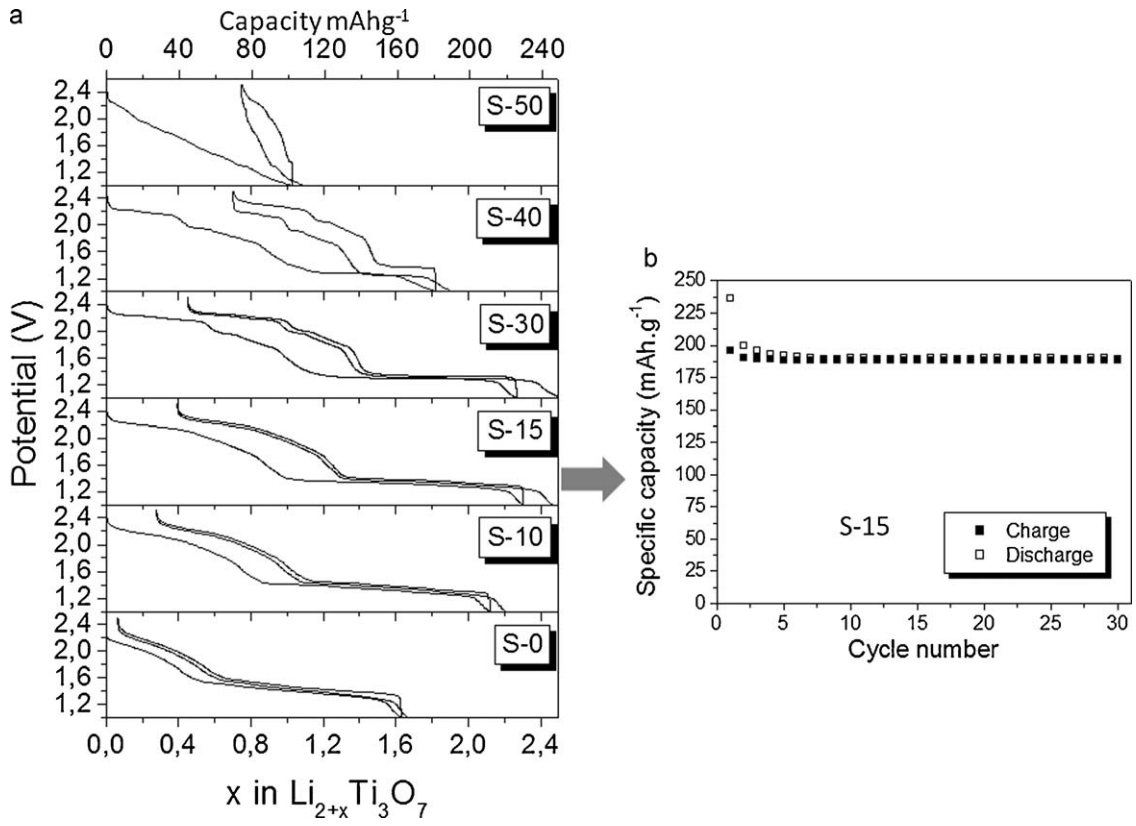

Fig. 6. (a) Galvanostatic curves of S-samples at *C*/10 cycling rate (1Li/10 h) and (b) the capacity retention of S-15 (C/10).

galvanostatic curve, the first part of the discharge from 2.5 and 1.5 V corresponds to the insertion of Li in the tetrahedral site in the center of channels, and the second part from 1.5 to 1 V to the insertion of Li the tetrahedral sites sharing a face with the TiO_6 of the network.

3.3.2. Li_xTiO_2 (R) ($0 \leq x < 0.57$))

In Fig. 6a the galvanostatic curves of the S-samples ($0 < S < 50$ wt% sucrose) give evidence of the evolution of the electrochemical behavior functions of the C content. The number of Li inserted is ranged from 0.1 to 2.1 Li per $Li_2Ti_3O_7$ formula unit for the S-50 to S-15 samples respectively, leading to capacities ranging from 20 to 190 mAh g^{-1}. The derivative curves (Fig. 7) allow better analysing the electrochemical processes and show strong modifications between the samples. S-15 and S-40 show much more narrow peaks than S-0. The curve of the latter presents a very broad peak centered at 2.1 V and the two peaks at 1.5 V and 1.4 V described above (T1 and T2 sites) and previously reported for $Li_2Ti_3O_7$ (R) [4,7]. The S-15 curve presents several broad peaks in the [2.5, 1.4 V] region and two peaks at lower potential i.e. 1.35 V and 1.3 V and the S-40 curve shows peaks well defined in the [2.5, 1.4 V] region and a single sharp peak at 1.27 V. It is noticeable that the S-40 curve is very similar to that reported for TiO_2 (R) [13]. The presence of numerous peaks clearly suggests that complex electrochemical processes take place in the 1.0–2.4 V region as previously described in the literature for TiO_2 (R) [4,13].

The transformation of the galvanostatic curve with increasing of C content is consistent with the progressive delithiation of the ramsdellite phase already demonstrated by the XRD analysis. Although the electrochemical process taking place during the discharge is the reduction of Ti^{4+} to Ti^{3+} in all ramsdellite phases (from $Li_2Ti_3O_7$ to TiO_2 (R)), the intercalation processes are unlike due to structural differences. In $Li_2Ti_3O_7$, following the structural model, part of the Ti positions are occupied by lithium atoms [12] and part of the Li occupy tunnel positions, while in the case of Li_xTiO_2 (R) the tunnels are partly ($0.57 < x < 0$) or fully ($x = 0$) empty. In the case of the series Li_xTiO_2 ($0 < x < 0.5$) only the T1 tetrahedral site is occupied by lithium ions up to a maximum of 50% as reported for $Li_{0.5}TiO_2$ [7,8]. The associated electrochemical curves show [13] several processes separated by more or less pronounced voltage drops. Lithium insertion process can be roughly divided into two regions which are characterized by distinct voltage ranges. Insertion of the first half of Li ions takes place over a wide voltage window, from 2.5 to 1.4 V, whereas insertion of the second half is achieved at a low constant voltage from 1.4 to 1.0 V. The first part is assigned to the maximum site occupation of the site T1 which cannot exceed 50% due to very short distances between the centers of adjacent face-sharing LiO_4 tetrahedron in the tunnel and the second part to the occupation of the still empty tetrahedral T2 site. Anyway structural work remains to be done to clarify the different processes on the first voltage region 2.5–1.4 V to fully understand the multiple small steps occurring on discharge.

The best reversible capacity 190 mAh g^{-1} and the best capacity retention (Fig. 6b) are measured for the S-15 sample while the capacity dramatically decreases for the samples with C content greater than 30%.

4. Discussion

The XRD patterns and the DTA of the carbonated samples synthesized with different contents of sucrose under Ar/H_2 with low or high flows have revealed the following: (i) the addition of sucrose in the precursors mixture under high Ar/H_2 flow produces structural modification of the ramsdellite $Li_2Ti_3O_7$, (ii) the refined cell parameters of the R phase are indicative of a progressive delithiation with increasing of residual C content; (iii) for an sucrose amount in the

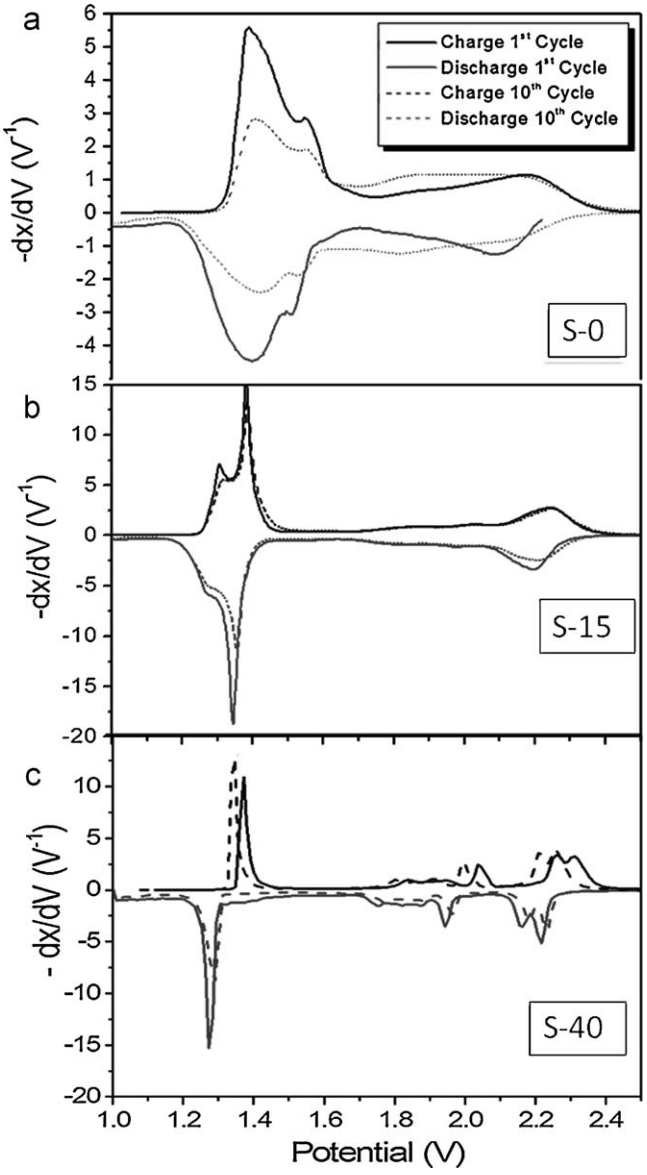

Fig. 7. Derivative curve of 1st and 10th cycles for the (a) S-0 ($Li_2Ti_3O_7$), (b) S-15 and (c) S-40 (TiO_2 R) samples.

synthesis higher than 30% the ramsdellite phase is fully delithiated and ascribable to the metastable TiO_2 R phase, and (iv) the progressive delithiation of the R phase is accompanied by the growth of a secondary phase ascribable to the cubic phase Li_2TiO_3. It can be deduced that under these specific synthesis conditions a Li_xTiO_2-R/Li_2TiO_3 composite (i.e. Li poor ramsdellite phase/Li rich cubic phase) is obtained and that the TiO_2 (R) metastable phase which is difficult to synthesize by other ways [8] is available by these synthetic conditions.

Although the electrochemical processes in S-40 is attributable to TiO_2 (R) the specific capacity is far from the theoretical capacity (335 mAh g^{-1}) corresponding to the insertion of 1 lithium per TiO_2 (R) mole. It can be attributable to the impossibility of Li atoms to occupy concomitantly both T1 and T2 sites. Moreover the additional phase Li_2TiO_3 formed when the C content increases is inactive vs. Li [14].

Fig. 8 presents both the capacity and the ratio ramsdellite/Li_2TiO_3 of the S-samples as function of the sucrose amount in the preparation. The ratio ramsdellite/Li_2TiO_3 has been estimated from the surface area peaks of the more intense XRD

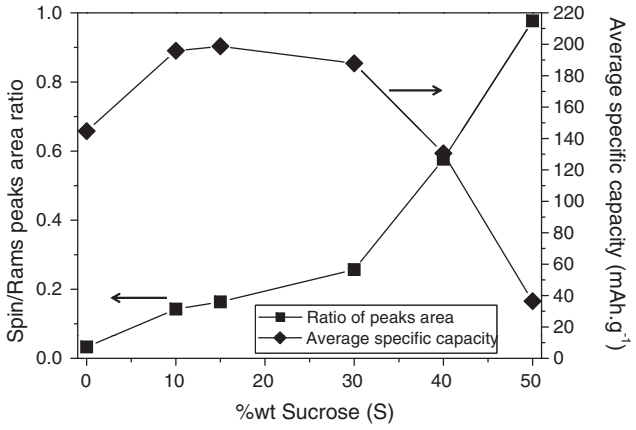

Fig. 8. Ratio ramsdellite/Li_2TiO_3 (spinel) and specific capacity in each S-sample as function of the sucrose amount in the S-sample preparations. The ratio ramsdellite/Li_2TiO_3 has been estimated from the surface area peaks of the more intense XRD peaks of each phase R/Li_2TiO_3.

peaks (at 20° and 43° for the R and the cubic phase respectively) of each phase. The best reversible capacity is obtained for the S-10 and S-15 samples (190 mAh g^{-1}) and is higher than the capacity of the standard (S-0) $Li_2Ti_3O_7$ phase 154 mAh g^{-1} (0.55 Li) demonstrating the benefit of the sucrose addition. For sucrose contents higher than 30% (residual C is higher than 5 wt% in the samples), the capacity dramatically fades. It means that the benefit brought by the increased lithium electrochemical insertion is hampered by the formation of Li_2TiO_3 inactive phase vs. lithium. As shown on Fig. 8, the best compromise between the formation of delithiated R phase with high theoretical capacity and the formation of the inactive Li_2TiO_3 is reached for a sucrose addition ranging from 10 to 30 wt%. Finally very interesting performances were obtained for the 15-sample with a 190 mAh g^{-1} capacity and a good capacity retention on cycling.

5. Conclusion

These original carbothermal synthesis allowed stabilizing the TiO_2 (R) metastable phase which is difficult to obtain by other ways and which presents very attractive theoretical capacity (335 mAh g^{-1}). By increasing the sucrose content in the precursor's mixture it is possible to progressively decrease the lithium amount in the Li_xTiO_2 (R). This trend is accompanied by the formation of a phase richer in Li and Ti, Li_2TiO_3. Unfortunately this latter is inactive vs. Li in the battery and a compromise between the amount of delithiated R phase with high theoretical capacity and the amount of the inactive Li_2TiO_3 is needed. By tailoring the percentage of carbonaceous additive, the nature of gas and the gas flow during the synthesis, we have succeed in the preparation of a titanate composite electrode providing high capacity. Needless to say investigations are now needed (i) to know the complete structure and composition in Li, C, O of the modified ramsdellite phase by both neutron diffraction and X-ray absorption investigations, (ii) to identify the location and nature of carbon and (iii) to deeply understand the electrochemical processes.

References

[1] A.M. Bystroèm, Acta Chem. Scand. 3 (1949) 163.
[2] J. Akimoto, Y. Gotoh, M. Sohma, K. Kawaguchi, Y. Oosawa, J. Solid State Chem. 110 (1994) 150.
[3] B. Morosin, J.C. Mikkelsen, Solid State Commun. 31 (1979) 741.
[4] M.E. Arroyo y de Dompablo, E. Moraân, A. Vaârez, F. Garcõâa-Alvarado, Mater. Res. Bull. 32 (1997) 993.
[5] R.K.B. Gover, J.T.S. Irvine, A.A. Finch, J. Solid State Chem. 132 (1997) 382.

[6] J. Akimoto, Y. Gotoh, Y. Oosawa, N. Nonose, T. Kumagai, K. Aoki, J. Solid State Chem. 113 (1994) 27.
[7] C. Villevieille, M. Van Thournout, J. Scoyer, C. Tessier, J. Olivier-Fourcade, J.-C. Jumas, L. Monconduit, Electrochim. Acta 55, 23, 30 (2010) 7080–7084.
[8] J. Rodriguez-Carvajal, Physica B 192 (1993) 55–69.
[9] Y. Takahashi, N. Kijima, J. Akimoto, Chem. Mater. 18 (2006) 748–752.
[10] J. Grins, A. West, J. Solid State Chem. 65 (1986) 265.
[11] I. Abrahams, P.G. Bruce, W.I.F. David, A.R. West, J. Solid State Chem. 78 (1989) 170.
[12] B. Morosin, J.C. Mikkelsen, Acta Crystallogr. B 35 (1979) 798.
[13] A. Kuhn, R. Amandi, F. Garcõâa-Alvarado, J. Power Sources 92 (2001) 221–227.
[14] P. Kubiak, Thesis, Université de Montpellier 2, France, 2003.